Cooperative Effect of Hydroxide and Fluorinated Organic Ions as Structure Directing Agent in the Synthesis of Crystalline Microporous Aluminophosphates†

Luis Gómez-Hortigüela,*[,‡,§] Carlos Márquez-Álvarez,[‡] Furio Corà,[§,||] Fernando López-Arbeloa,[⊥] and Joaquín Pérez-Pariente[‡]

Instituto de Catálisis y Petroleoquímica (ICP), CSIC, Marie Curie 2, Cantoblanco, 28049 Madrid, Spain, Davy Faraday Research Laboratory, The Royal Institution of Great Britain, 21 Albemarle Street, London W1S 4BS, United Kingdom, Department of Chemistry, University College London, 20 Gordon Street, London WC1H 0AJ, United Kingdom, and Departamento de Química Física, Universidad del País Vasco-EHU, Apartado 644, 48080 Bilbao, Spain

Received March 28, 2007. Revised Manuscript Received July 31, 2007

A combination of computational methods based on molecular mechanics, fluorescence, FTIR and magic-angle spinning NMR spectroscopies, and thermogravimetric analysis coupled with mass spectrometry have been employed to explain the structure directing effect of dibenzyldimethylammonium (dbdm) and its bis(*ortho*- and *meta*-fluorobenzyl) derivatives in the synthesis of aluminophosphates with AFI-type structure. We identify a supramolecular assembly of dbdm cations with hydroxide anions which compensate for their positive charge. These hydroxide anions appear to be also coordinated to framework aluminum atoms, bridging the organic SDAs and the framework walls. Such assembly is most promoted when the fluorine atom is located in the ortho position of the aromatic ring, which considerably enhances the electrostatic interaction with the inorganic network. The presence of the OH^- counterion provides charge balance for the ortho-fluorinated SDA and leads to fewer framework defects. In the other cases, most of the positive charge of the dbdm cations is instead compensated by the presence of framework defects.

Introduction

Since their discovery, microporous materials have been widely employed in applications such as molecular sieving and ion-exchange,[1–3] which exploit the molecular dimensions and the crystalline nature of the microporous structure to discriminate between molecules with very small steric differences. In addition, crystalline microporous materials can be synthesized in different compositions, several of which have useful catalytic properties. Microporous aluminophosphates (AlPOs) were first reported by Wilson et al.[4] and have been widely studied since. The synthesis of microporous materials is based on hydrothermal methods, where the source of the inorganic ions, water, and, generally, an organic molecule are heated in an autoclave for a time ranging from a few hours to weeks.[5–7] The role of the organic molecules, which are also called structure directing agents (SDAs), has been usually described as a "template effect",[8] to indicate that the organic molecules organize the inorganic tetrahedral units into a particular topology around themselves during the nucleation process, providing the initial building blocks for further crystallization of the microporous structure. Nevertheless, the exact role of the SDA molecules is still not fully understood.[9] These organic molecules are encapsulated inside the microporous network during its crystallization and thus contribute to the stability of the system. Although a true templating effect has been occasionally found (the main example is a triquaternary ammonium cation inside the ZSM-18 zeolite[10]), the structure directing effect is not as specific as expected. Experimental evidence clearly shows that the gel chemistry and kinetic factors can also have a critical bearing on the nature of the microporous material formed.

The ability of a molecule to direct the crystallization of a certain microporous structure depends mainly on the nonbonding interactions established between them.[11–14] Our recent work has demonstrated that a change in the chemical nature of such interactions can considerably alter the structure

† Part of the "Templated Materials Special Issue".

* Corresponding author: e-mail: lhortiguela@icp.csic.es.
‡ Instituto de Catalisis y Petroleoquimica.
§ The Royal Institution of Great Britain.
|| University College London.
⊥ Universidad del País Vasco-EHU.

(1) Davis, M. E. *Acc. Chem. Res.* **1993**, *26*, 111.
(2) Naber, J. E.; de Jong, K. P.; Stork, W. H. J.; Kuipers, H. P. C. E.; Post, M. F. M. *Stud. Surf. Sci. Catal.* **1994**, *84C*, 2197.
(3) Venuto, P. B. *Microporous Mesoporous Mater.* **1994**, *2*, 297.
(4) Wilson, S. T.; Lok, B. M.; Flanigen, E. M. U.S. Patent 4,310,440, 1982.
(5) Lok, B. M.; Cannan, T. R.; Messina, C. A. *Zeolites* **1983**, *3*, 282.
(6) Davis, M. E.; Lobo, R. F. *Chem. Mater.* **1992**, *4*, 756.
(7) Zones, S. I.; Nakagawa, Y.; Lee, G. S.; Chen, C. Y.; Yuen, L. T. *Microporous Mesoporous Mater.* **1998**, *21*, 199.
(8) Gies, H.; Marler, B. *Zeolites* **1992**, *12*, 42.
(9) Lobo, R. F.; Zones, S. I.; Davis, M. E. *J. Inclusion Phenom. Mol. Recognit. Chem.* **1995**, *21*, 47.
(10) Lawton, S. L.; Rohrbaugh, W. J. *Science* **1990**, *247*, 1319.
(11) Lewis, D. W.; Freeman, C. M.; Catlow, C. R. A. *J. Phys. Chem.* **1995**, *99*, 11194.
(12) Sastre, G.; Cantin, A.; Díaz-Cabañas, M. J.; Corma, A. *Chem. Mater.* **2005**, *17*, 545.
(13) Sastre, G.; Leiva, S.; Sabater, M. J.; Giménez, I.; Rey, F.; Valencia, S.; Corma, A. *J. Phys. Chem. B* **2003**, *107*, 5432.
(14) Nakagawa, Y.; Lee, G. S.; Harris, T. V.; Yuen, L. T.; Zones, S. I. *Microporous Mesoporous Mater.* **1998**, *22*, 69.

10.1021/cm070855b CCC: $40.75
Published on Web 12/01/2007

directing ability of the organic molecules.[15] From a combination of experimental and theoretical approaches, we have studied the influence of including fluorine atoms in the organic molecules which act as SDAs in all-silica zeolite[16] and AlPO systems.[17,18] Up to date, we have found several effects associated with the presence of fluorine atoms in the SDA molecules. In general, fluorine increases the interaction between the SDA molecules and the inorganic networks and thus improves the structure directing ability of the molecules. This effect is due to an enhanced electrostatic interaction arising from the polarized C−F bond.[18] However, fluorine can affect the packing ability of the molecules inside the microporous structure, resulting in either increase or reduction of the template density, depending on the position of fluorine in the molecule and the intermolecular orientation in the actual system examined. A cooperative structure directing effect between the fluorinated organic molecules and fluoride anions has been found in the crystallization of the EUO-type structure, where the electrostatic interaction with the fluoride ions determines the orientation of the fluorinated SDA molecules inside the microporous structure.[16] Finally, it was demonstrated that fluorine can influence the dopant incorporation and ordering in the microporous network.[19,20]

Within this effort, we have recently discussed the effect that the presence of fluorine atoms in the different positions of both aromatic rings of the dibenzyldimethylammonium (dbdm) cation has in the synthesis of AlPO-5 and SAPO-5 (AFI-type structure).[21] This microporous structure is composed of unidirectional noninterconnected 12-member ring (MR) channels, surrounded by smaller 6 and 4MR channels. Experimental results showed that the presence of fluorine atoms in any of the positions of both aromatic rings in the dbdm cation improved its structure directing ability (see Figure 1 in Supporting Information). Modeling work further indicated that the dbdm cations form a supramolecular arrangement as chains in which the benzyl rings of consecutive molecules overlap, and the two benzyl rings of the same molecule are nearly perpendicular to each other.[22] As a result of the formation of such an assembly, dbdm is incorporated in the AFI framework at a density as high as one molecule per unit cell. Including fluorine atoms in any of the positions of the aromatic rings did not affect the packing ability; the presence of fluorine in meta or para positions increased the electrostatic interaction with the structure, in agreement with experiments.[21] However, fluorine in the ortho position decreased the interaction energy of the SDA with the AFI structure, suggesting a lower structure directing ability, in contrast with the experimental results. Thus, the high structure directing efficiency of the ortho-fluorinated derivative of dbdm to direct the synthesis of the AFI structure found experimentally cannot be explained computationally when the calculations only take the SDA molecules into account. This result may indicate the exclusion of some important variable from the computational models, a topic that we investigate in the present paper.

Two factors may be of importance: First, the occlusion of the organic cations, such as dbdm, brings the requirement of compensating their positive charge to achieve charge neutrality. The most common way of achieving this goal is introducing in the synthesis medium low valent dopant ions, such as Mg^{2+}, which introduce a negative charge in the AlPO framework when they isomorphically replace Al^{3+}. Another well-known mechanism of charge compensation is the incorporation of extraframework anions (e.g., fluoride) in the forming solid. In the absence of these species from the synthesis, charge compensation comes from negatively charged intrinsic framework defects (such as $-O^-$ or cation vacancies) in the inorganic network. Second, the templated synthesis of AFI is carried out in aqueous media; water molecules can therefore be occluded in the microporous structure during the synthesis, and in this case their interaction with the inorganic network contributes to the energy balance of the system. The importance of water in the synthesis of microporous materials has been recently pointed out by Férey and co-workers for the Zn-AlPO framework MIL-74.[23] The incorporation of hydroxide anions, OH^-, should in this case also be considered as a viable charge balancing mechanism.

Therefore, in the present work we extend previous studies by examining computationally and experimentally the inclusion of hydroxide anions and/or water molecules in the dbdm−AFI system. As we shall see, their contribution explains the different structure directing ability of the fluorinated dbdm derivatives, in agreement with experimental evidence. As reported in ref 21, the use of the para-fluorinated dbdm molecule as SDA led to the crystallization of AlPO-5 together with traces of another phase which could not be identified (see Figure 1, Supporting Information). Therefore, because of the additional difficulty when assigning the different Fourier transform infrared (FTIR) bands caused by the presence of an unknown phase, we performed the study only for the ortho-, meta- and nonfluorinated dbdm molecules, where we could assign all the different bands to the AFI material.

Computational Details

A detailed description of the computational methodology employed is given in our previous work.[21] The geometry of the AFI structure was optimized with the GULP code[24] and the interatomic potentials from Gale and Henson,[25] and it

(15) Pérez-Pariente, J.; Gómez-Hortigüela, L.; Arranz, M. *Chem. Mater.* **2004**, *16*, 3209.
(16) Arranz, M.; Pérez-Pariente, J.; Wright, P. A.; Slawin, A. M. Z.; Blasco, T.; Gómez-Hortigüela, L.; Corà, F. *Chem. Mater.* **2005**, *17*, 4374.
(17) Gómez-Hortigüela, L.; Pérez-Pariente, J.; Blasco, T. *Microporous Mesoporous Mater.* **2005**, *78*, 189.
(18) Gómez-Hortigüela, L.; Corà, F.; Catlow, C. R. A.; Pérez-Pariente, J. *J. Am. Chem. Soc.* **2004**, *126*, 12097.
(19) Gómez-Hortigüela, L.; Márquez-Álvarez, C.; Sastre, E.; Corà, F.; Pérez-Pariente, J. *Catal. Today* **2006**, *114*, 175.
(20) Gómez-Hortigüela, L.; Corà, F.; Catlow, C. R. A.; Pérez-Pariente, J. *Phys. Chem. Chem. Phys.* **2006**, *8*, 486.
(21) Gómez-Hortigüela, L.; Corà, F.; Catlow, C. R. A.; Blasco, T.; Pérez-Pariente, J. *Stud. Surf. Sci. Catal.* **2005**, *158A*, 327.
(22) Gómez-Hortigüela, L.; Pérez-Pariente, J.; Corà, F.; Catlow, C. R. A.; Blasco, T. *J. Phys. Chem. B* **2005**, *109*, 21539.
(23) Henry, M.; Taulelle, M.; Loiseau, T.; Beitone, L.; Férey, G. *Chem.—Eur. J.* **2004**, *10*, 1366.
(24) Gale, J. D. *J. Chem. Soc., Faraday Trans.* **1997**, *93*, 629.
(25) Gale, J. D.; Henson, N. J. *J. Chem. Soc., Faraday Trans.* **1994**, *90*, 3175.

remained fixed during the calculations. Molecular structures and the interaction energies of the SDAs with the framework were described with the CVFF forcefield,[26] in which the van der Waals and electrostatic interactions are explicitly included. The atomic charges for the dbdm cations (total molecular charge of +1) were calculated by the charge-equilibration method.[27] The net molecular charge of +1 had to be compensated by the inorganic framework. In the case where the hydroxide anions were included in the network, the presence of these anions provided the charge balance. However, in the study of the systems in the absence of hydroxide anions, we employed a charge-balance model that makes reference to the "uniform charge background" method,[28] where charged defects are compensated by a uniform distribution of charge across the whole structure. Therefore, the charges for the framework atoms were –1.2000, 1.4000, and 3.3167 for oxygen, aluminum and phosphorus to provide charge balance. The atomic charges for the water molecules were −0.82 and +0.41 for oxygen and hydrogen, respectively. These values are used in the cvff parametrization, which has been shown to describe well the properties of water containing systems.[29] Finally, the atomic charges for the hydroxide anions were −1.61 and 0.61 for oxygen and hydrogen, respectively.

The initial models were those accounting for the equilibrium disposition of dbdm and its fluoro-derivatives in the AFI channels, described in earlier work.[21] The systems were composed of four SDA molecules in a $1 \times 1 \times 4$ supercell of the AFI structure, consistent with the stable packing of one molecule per unit cell and relative orientation of the molecules. In the optimum configuration of the SDA cations, obtained after simulated annealing, the two aromatic rings of the same molecule form a nearly perpendicular angle. Starting from these systems, water molecules were inserted in the structure using a grand canonical (pVT ensemble) Monte Carlo (MC) procedure, where Coulomb interactions were explicitly included. In these calculations, the coordinates of both the AFI structure and the organic molecules were kept fixed. A total of 2.5 million configurations were sampled, with a constant water partial pressure of 100 kPa (∼1 atm). This first set of calculations gave us an idea of how the different dbdm derivatives interact with adsorbed small molecules such as water. The geometry of the SDAs and water was varied by energy minimization after the insertion of water.

After the experimental study, a set of additional calculations was carried out including hydroxide anions in the systems. They were manually inserted in the required positions, the systems were relaxed, and the interaction energies were calculated by simulated annealing followed by energy minimization (in these calculations both SDA and hydroxide anions were allowed to relax). The total interaction energies were calculated by subtracting the energy of the isolated molecules from the energy of the interacting system.

Experimental Details

Synthesis and characterization of both the SDAs and the microporous materials are detailed in our previous work.[21]

Solid state UV–visible fluorescence spectra were recorded in the 270–600 nm range after excitation at 260 nm in a SPEX fluorimeter model Fluorolog 3-22 equipped with a double monochromator in both the excitation and the emission channels and a red-sensitive photomultiplier detector operating with a Peltier cooling system. The fluorescence spectra were registered in the front-face configuration in which the emission signal was detected at 22.5° with respect to the excitation beam. To collect the spectra of the crystalline AlPO, a thin film was deposited on a glass slide by solvent evaporation from a dichloromethane suspension.

Chemical analyses (C, H, N) were performed on a Perkin-Elmer 2400 CHN analyzer. Thermogravimetric analysis (TGA) studies were performed from 30 to 1000 °C in a Perkin-Elmer TGA7 instrument, coupled with a mass spectrometer for evolved gas analysis, under a helium atmosphere. The heating rate was 20 °C/min, and the helium flow was approximately 100 mL/min. The gases generated from the TGA were analyzed with a Fisons MD-800 mass spectrometer, connected to the TGA instrument through an interface provided by Perkin-Elmer, which permits the sample amount that goes to the ionization chamber of the mass spectrometer to be optimized. The ionization potential employed was 70 eV, with a 6 scan/min frequency and an atomic mass range of 2–200 amu.

Infrared spectra were recorded using a Nicolet 5ZDX FTIR spectrometer provided with an MCT detector. Spectra in the 4000–1000 cm^{-1} wavenumber range were acquired at 4 cm^{-1} resolution by averaging 250 scans, using Happ−Genzel apodization. The samples were pressed into thin self-supporting wafers (thickness ca. 8 mg/cm^2), introduced in an IR cell provided with CaF_2 windows and dehydrated under dynamic vacuum (10^{-3} Pa) prior to analysis. The dehydration treatment was carried out successively at room temperature for 1 h, 80 °C for 1 h and 150 °C for 10 min, with heating ramps of 5 °C/min.

The ^{27}Al MAS NMR spectra were recorded with a Bruker AV 400 WB spectrometer, using a BL7 probe. These ^{27}Al spectra were measured using pulses of 1 μs to flip the magnetization $\pi/12$ rad, with delays of 1 s between two consecutive pulses. The spectra were recorded while spinning the samples at approximately 11 kHz.

Results and Discussion

Henceforth, the AFI structure synthesized with the different SDA cations will be denoted as dbdm (synthesized with dibenzyldimethylammonium), ooFFdbdm (with bis(*ortho*-fluorobenzyl)dimethylammonium) and mmFFdbdm (with bis(*meta*-fluorobenzyl)dimethylammonium).

1. Supramolecular Chemistry of the SDAs: Experimental Evidence. A crucial feature in the arrangement of the dbdm-based SDAs inside the channels, revealed in our modeling work as discussed in the Introduction, is the formation of supramolecular assemblies in which the benzyl rings of adjacent molecules ovelap, leading to a long-range ordered chain. To verify experimentally the existence of this supramolecular assembly, two characterization techniques were employed, namely chemical analysis and UV–visible fluorescence spectroscopy. The former resulted in an organic

(26) Dauger-Osguthorpe, P.; Roberts, V. A.; Osguthorpe, D. J.; Wolff, J.; Genest, M.; Hagler, A. T. *Proteins: Struct., Funct., Genet.* **1988**, *4*, 21.
(27) Rappe, A. K.; Goddard, W. A., III *J. Phys. Chem.* **1995**, *95*, 3358.
(28) De Vita, A.; Gillan, M. J.; Lin, J. S.; Payne, M. C.; Stich, I.; Clarke, L. J. *Phys. Rev. B* **1992**, *46*, 12964.
(29) Williams, J. J.; Smith, C. W.; Evans, K. E.; Lethbridge, Z. A. D.; Walton, R. I. *Chem. Mater.* **2007**, *19*, 2423.

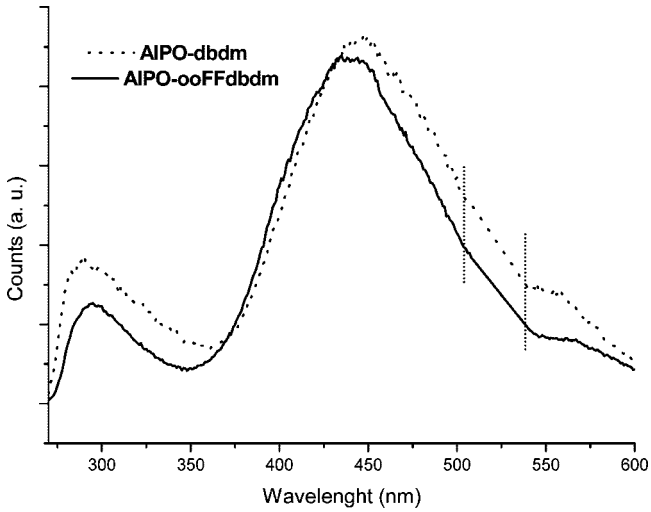

Figure 1. Solid state fluorescence spectra of AlPO-5 samples synthesized with dbdm (dashed line) and ooFFdbdm (solid line) SDAs after excitation at 260 nm. An extremely intense signal coming from the first harmonic of the excitation wavelength observed at 520 nm has been removed (range between dashed lines).

content of 0.9 and 1.0 SDA molecules in each unit cell for dbdm and ooFFdbdm samples, respectively. The length of the dbdm molecule, as measured in the most stable conformation in vacuum (calculated by the DFT methodology), is 12.12 Å, while the length of the AFI unit cell along the 12MR channel is 8.48 Å. If no overlapping of the aromatic moieties occurred, the density of SDAs would be at most of 0.7 molecules per unit cell. The high values of organic content inside the AFI structure observed experimentally cannot be reached unless the benzyl rings of consecutive SDA molecules overlap, leading to the formation of supramolecular aggregates. This result provides a first indirect evidence for the formation of supramolecular assemblies of the dbdm cations. The existence of such aggregates was further confirmed by solid state fluorescence spectroscopy. Emission of monomeric aromatic moieties usually occurs at approximately 290 nm; however, aggregation of such aromatic molecules leads to a reorganization of the excited energetic levels which results in the appearance of a new emission band shifted to longer wavelengths.[30,31] Figure 1 shows the UV–visible fluorescence spectra of dbdm and ooFFdbdm samples, after excitation at 260 nm. Two bands can be clearly observed in both cases, one centered at around 290 nm and another at 440 nm, which correspond to dbdm SDA molecules as monomer and aggregates, respectively. The high intensity of the hypsochromic emission band (higher than the monomer emission) clearly confirms the presence of supramolecular aggregates in both samples.

2. Inclusion of Molecules in the Channels in Addition to the SDAs: Computational Hypothesis. As discussed earlier, the interaction energy of the three SDA molecules with the AFI framework does not correlate with their structure directing efficiency. We have therefore employed a new set of calculations to refine our computational model. Upon analysis of the SDA location, we realized that in the 12MR channels of the AFI structure filled by the dbdm supramolecular assemblies, some empty space is left in the region surrounding the two methyl substituents of the central ammonium ion. The dimensions of this empty space allow additional small species present in the synthesis medium to be hosted, such as water molecules or hydroxide ions. The F substituents on the benzyl groups are also in close proximity, so that they can influence the number and type of species that can be hosted in such a space. We have investigated this topic computationally, initially employing water molecules as the occluded species.

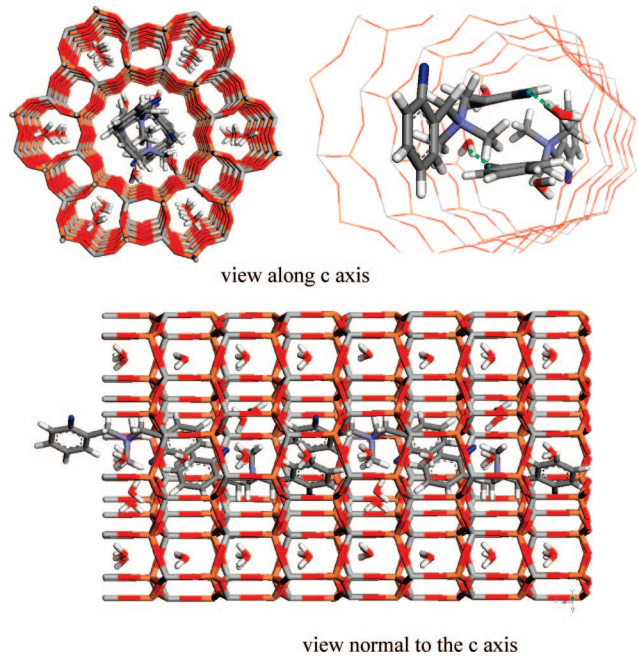

Figure 2. Location of water molecules in the ooFFdbdm system after the MC simulation at a pressure of 100 kPa. Two views of the AFI channel are presented (top-left and bottom). Top-right: water and organic molecules inside the 12MR channel, highlighting the fluorine−water interaction (dashed green line). Fluorine atoms are displayed in dark blue.

Figure 2 shows the incorporation of water molecules in the ooFFdbdm system after the MC docking simulation. Water molecules fill the 6MR channels of the AFI structure, incorporating four molecules in each unit cell (16 molecules in the $1 \times 1 \times 4$ supercell); the 4MR channels are instead too small to accommodate water. In addition, water molecules are loaded in the main channel, close to the ooFFdbdm cations, incorporating two molecules per SDA cation (eight molecules in total in the $1 \times 1 \times 4$ supercell: Figure 3, top). These water molecules are located near the nitrogen and fluorine atoms of the ooFFdbdm molecules. The total content of water for this sample corresponds to six molecules each unit cell.

The mmFFdbdm system showed similar behavior: four water molecules per unit cell were incorporated in the 6MR channels, while seven were loaded in the $1 \times 1 \times 4$ supercell in the 12MR channels. This result indicates a slightly lower water incorporation in the mmFFdbdm system compared to ooFFdbdm. Very different values are instead found for dbdm: the 6MR channels are fully loaded with water molecules in the same way as for the other two systems; however, only four water molecules were loaded in the 12MR channel of

(30) Hashimoto, S.; Ikuta, S.; Asahi, T.; Masuhara, H. *Langmuir* **1998**, *14*, 4284.
(31) Corma, A.; Rey, F.; Rius, J.; Sabater, M. J.; Valencia, S. *Nature* **2004**, *432*, 287.

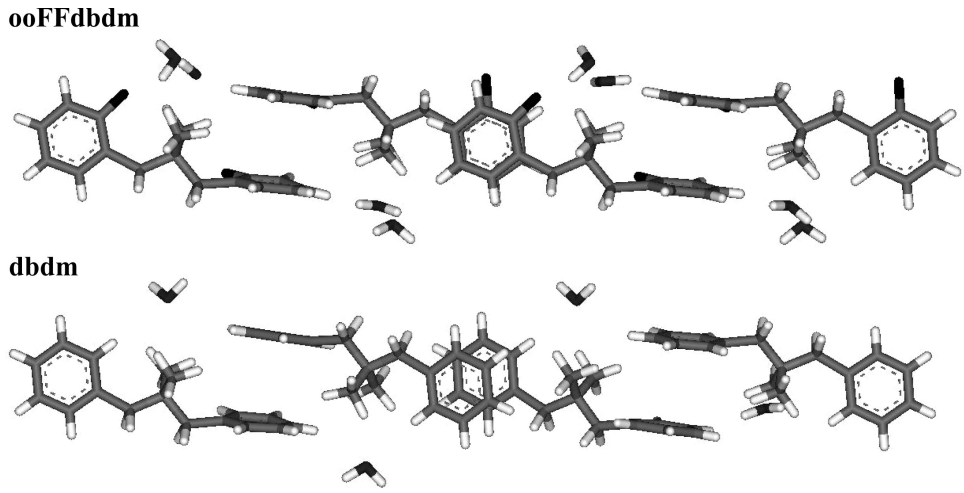

Figure 3. Location of water molecules inside the 12MR channel in the ooFFdbdm (top) and dbdm (bottom) systems after the MC simulation at a pressure of 100 kPa. AFI atoms are omitted for clarity. Fluorine atoms are displayed in black.

the $1 \times 1 \times 4$ supercell. Figure 3 (bottom) shows the location of these water molecules in the main channel of the dbdm system. These results suggest that the interaction of the water molecules with the nonfluorinated and the meta-fluorinated derivatives in the main channel is lower than that with ooFFdbdm, as confirmed by the calculated interaction energies between water and SDAs, which were found to be 8.8, 15.8, and 20.1 kcal/mol for dbdm, mmFFdbdm, and ooFFdbdm, respectively. The higher interaction of the ooFFdbdm molecules with the water molecules in the 12MR channel is due to the development of H-bonds between negatively charged fluorine atoms of the SDA and positively charged hydrogen atoms of the water. In the case of ooFFdbdm, the F substituents point toward a region of the 12MR channel left unoccupied by the SDA self-assembly, where water can be easily accommodated and oriented in an H-bonding configuration with F. This also occurs in the mmFFdbdm SDA, although the larger distance between *meta*-fluorine (distance F···O is 2.5 Å when fluorine is in the ortho position and 4.4 Å when it is in meta) and water reduces the effectiveness of the H-bonds; nevertheless, the electrostatic field generated by fluorine yields an appreciable electrostatic interaction energy with water. Finally, in dbdm the hydrophobic nature of the benzyl ring without polar substituents prevents (or reduces) the inclusion of water in its vicinity. These results demonstrate the possibility of including water together with the organic molecules, close to their ammonium moieties, in the AFI structure. In addition, the closer distance of fluorine when located in the ortho position leads to a higher interaction with the water molecules in the 12MR channels. This higher water loading in the ooFFdbdbm sample could in principle explain its experimentally observed higher structure directing ability.

3. Inclusion of Molecules in the Channels in Addition to the SDAs: Experimental Verification. The result of the computational work observed in point 2 above prompted us to search for experimental confirmations of the presence of molecules other than the dbdm SDAs inside the structure. As mentioned in the Introduction, in principle two different kind of species could be occluded during the crystallization of the AlPO network from aqueous solutions: water molecules or hydroxide anions. We therefore performed an experimental study based on TGA coupled to mass spectrometry (MS), searching for a water desorption pattern which could confirm the presence of water derivatives (water or hydroxide anions) occluded in the AFI frameworks. Desorption of water molecules at high temperatures could indicate not only the presence of water molecules occluded within the organic SDAs but also of hydroxide anions, which would be protonated prior to their desorption as water. It is useful to compare the present results for dbdm SDAs with a system that does not contain small species in the 12MR channel; to this goal, we shall employ as reference an AFI sample obtained with benzylpyrrolidinium (bp) as the SDA.[17,18] An MC docking showed that in this case the inclusion of small species, like water, in the 12MR channel is not possible because of the very efficient space-filling of bp, which leaves no void space in the 12MR channel. Water molecules were inserted only in the 6MR channels.[32]

Figure 4 shows the TGA/MS results for ooFFdbdm and bp systems. The maximum desorption rate for the two SDA molecules occurs at ~350 °C (Figure 4, top). The most intense signals in the MS spectra of the evolved gases were observed at $m/z = 109$ and 91, originating from the $F-Ph-CH_2^+$ and $Ph-CH_2^+$ fragment ions corresponding to the ooFFdbdm and bp molecules, respectively, and at $m/z = 18$, due to water. These signals have been selected to track the losses of the SDA cations and water with increasing temperature, shown at the bottom of Figure 4. In the AlPO-5−bp system, where the modeling work indicates that no water is present in the 12MR channel, desorption of water occurs only at temperatures around 100 °C. We suggest that this desorption corresponds to water from the 6MR channels. However, in the ooFFdbdm case, in addition to the desorption at low temperatures (~100 °C) discussed earlier, another clear weight loss assigned to water desorption is observed simultaneously to the desorption/decomposition of the ooFFdbdm molecules. We tentatively assign this high-temperature water desorption to water molecules or hydroxide anions occluded

(32) Gómez-Hortigüela, L. Ph.D. Thesis, Instituto de Catalisis y Petroleoquimica (CSIC) and Universidad Autonoma de Madrid, Spain, 2006.

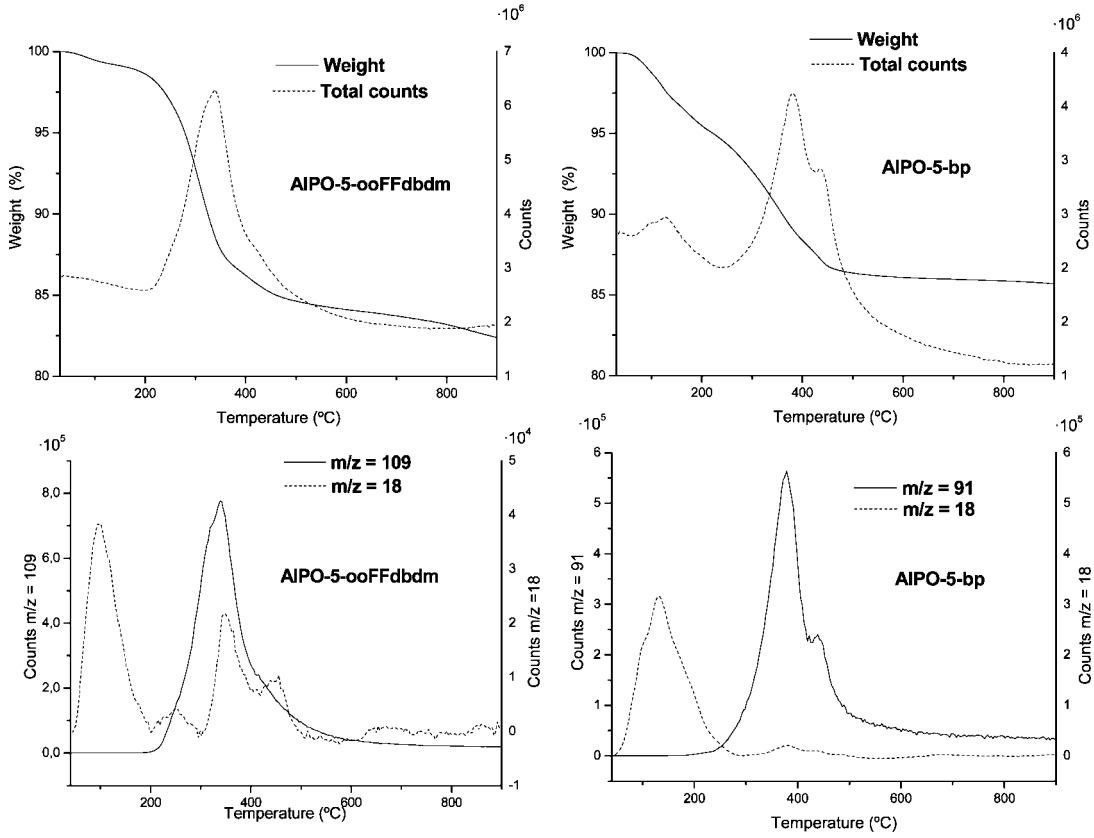

Figure 4. TGA/MS analysis of AlPO-5 samples synthesized with ooFFdbdm (left) and bp (right) SDAs. Top: percent of residual weight and MS total counts. Bottom: MS counts for selected m/z values representative of SDA fragment ions (m/z = 109 for ooFFdbdm and 91 for bp) and water (m/z = 18); a six points baseline was used.

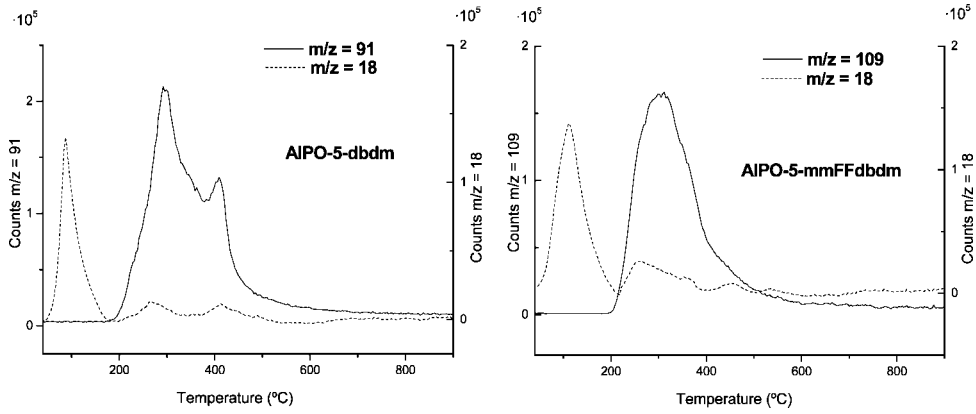

Figure 5. TGA/MS analysis of AlPO-5 samples synthesized with dbdm (left) and mmFFdbdm (right) SDAs, showing the MS signal intensity at m/z = 18 (water) and 91 (dbdm) or 109 (mmFFdbdm). A six points baseline was used.

within the organic molecules in the main channel, whose desorption occurs simultaneously to the loss of the organic molecules. In principle, the increase of the MS signal at m/z = 18 at high temperature could be also attributed to dehydroxilation processes associated to the organic desorption. However, this feature would be common to both bp and dbdm SDAs; because it was not observed in the bp system nor in the dbdm system (see below), we assign the water desorption at 350 °C to water or hydroxide species occluded in the 12MR channel and associated to the ooFFdbdm molecules. Note that TGA/MS data do not allow water and hydroxide to be differentiated, because hydroxide anions would also desorb as water after protonation.

The same TGA/MS experiment was carried out for the dbdm and mmFFdbdm systems. The MS signal intensities of both the SDA (m/z = 91 for dbdm and 109 for mmFFdbdm) and water (m/z = 18) are shown in Figure 5. A clear water desorption peak is found in all cases at low temperatures (~100 °C), coming from the desorption of water from the 6MR channels. A small desorption of water simultaneous to the SDA loss is also observed. The amount of water desorbed follows the order ooFFdbdm > mmFFdbdm > dbdm, consistent with the order of water content found computationally.

4. Nature of the Molecules Occluded: FTIR Experiments. Following the TGA work, which confirmed the presence of occluded water derivatives, we performed an

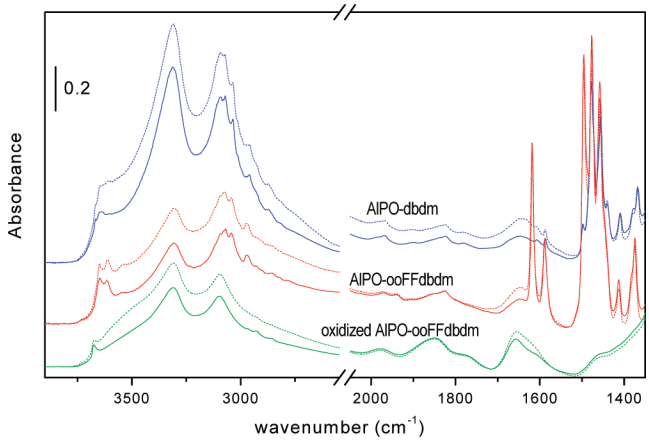

Figure 6. FTIR spectra after dynamic vacuum treatment at room temperature for 1 h (dotted lines) and at 150 °C for 10 min (solid lines) of AlPO-5 samples obtained with dbdm (blue, top) and ooFFdbdm (red, middle) SDAs. FTIR spectra of the latter AlPO-5 sample after template removal by low temperature oxidation with ozone are also shown in green (bottom).

FTIR study to clarify the chemical nature of the species released as water at high temperature. Infrared spectra of AlPO-5 samples obtained with the different dbdm derivatives were recorded after dynamic vacuum treatment at room temperature for 1 h and at 150 °C for 10 min. Figure 6 shows the spectra of the samples obtained with the dbdm cation (in blue) and the ortho-fluorinated dbdm cation (in red). The spectra for the meta-fluorinated compound are very similar to those of the dbdm sample, with only the expected changes in the low frequency region of the spectra for bands characteristic of the organic SDA, and, therefore, are not shown for clarity. The spectra obtained for the ooFFdbdm system after ex situ SDA removal by oxidation of the sample at low temperature (200 °C) under an ozone stream are also shown (in green). The presence of a small amount of adsorbed water in the samples evacuated at room temperature is assessed by a very broad absorption ranging from 3000 to 3600 cm^{-1} in the HOH stretching region and the bending band observed at approximately 1640 cm^{-1}. The spectra of Figure 6 show that most of the water molecules initially present in the samples (which produce very strong absorption in these two regions of the spectra for the nonevacuated samples) were removed after evacuation at room temperature for 1 h. The removal of molecular water was complete for the samples evacuated at 150 °C, as the remaining broad absorption that can be observed in the HOH bending region arises from combination modes of the AlPO network. These results evidence that molecular water is not retained at temperatures higher than 150 °C and indicate that the desorption of water molecules at high temperatures (∼350 °C) previously observed for the ooFFdbdm sample in the TGA/MS experiments is associated with the presence of hydroxide anions.

On the other hand, the intensity of infrared bands corresponding to organic matter (narrow bands in the regions 1350–1650 and 2850–3100 cm^{-1}) does not change along the degassing treatment (Figure 6), indicating that there is no loss of organic matter at temperatures below 150 °C, in agreement with what was previously concluded from the TGA/MS results.

In addition to the infrared bands discussed above, two intense broad bands centered at around 3310 and 3100 cm^{-1} can be observed in the FTIR spectra. The intensity of these bands does not change with the different evacuation treatments and, furthermore, they are not affected by the low temperature ozone oxidation treatment. To our knowledge, these two bands have not been reported in other FTIR spectra of microporous AlPO materials. They cannot correspond to coordinated water, because this should be desorbed by vacuum treatment at 150 °C. Their broadness and low frequency suggest a tentative assignment of these two bands to strongly interacting OH groups. Such hydroxyl species could be associated to framework defects, probably related to the presence of O^- species in the network. The FTIR spectra therefore indicate a much higher concentration of OH defects in the samples obtained with the nonfluorinated and meta-fluorinated SDAs, compared to the one obtained with the ortho-fluorinated SDA.

Finally, important differences can be found among the samples in the wavenumber region above 3500 cm^{-1}. The spectra of the sample oxidized with ozone exhibits a single band at 3673 cm^{-1}, which corresponds to isolated terminal POH groups in AlPO materials.[33] The spectra of the SDA-containing samples, however, do not show this band and exhibit additional features at lower frequency. A doublet at 3667/3643 cm^{-1} is observed for the dbdm material. In the sample obtained with the ortho-fluorinated cation, these two bands have a much higher intensity, and in addition, they are red-shifted approximately 20 cm^{-1} (3647/3617 cm^{-1}). In the case of the AlPO−mmFFdbdm system, a similar situation as for the nonfluorinated cation was found (see Figure 2, Supporting Information). This doublet has been previously assigned in the literature to hydroxide anions present in AlPO materials, whose presence is required to compensate the positive charge of the protonated triethylamine molecule, which acts as SDA.[34,35] These two bands appear in the spectra of the sample obtained with the nonfluorinated SDA, although their intensity is rather low. These bands are retained after the high temperature vacuum treatment but dissappear after the oxidation treatment, which seems to indicate that they are closely associated to the presence of the organic matter. On the basis of these grounds, we assign these two bands to hydroxide anions compensating the positive charge of the dbdm cations. The red-shift of these bands in the AlPO−ooFFdbdm system suggests a weaker O−H bond due probably to an interaction with the organic cation.

In summary, two different situations have been observed. In the AlPO−dbdm and −mmFFdbdm systems, there is a high concentration of OH groups associated to framework defects (broad bands at 3100 and 3310 cm^{-1}) and a low concentration of hydroxide anions (narrow bands at ∼3650 cm^{-1}). The opposite is found for the ortho-fluorinated dbdm cation, where there is a lower concentration of framework

(33) Montoya-Urbina, M.; Cardoso, D.; Pérez-Pariente, J.; Sastre, E.; Blasco, T.; Fornés, V. *J. Catal.* **1998**, *173*, 501.
(34) Popescu, S.; Thomson, S.; Howe, R. *Phys. Chem. Chem. Phys.* **2001**, *3*, 111.
(35) Schnabel, K.-H.; Finger, G.; Kornatowski, J.; Loffler, E.; Peuker, C.; Pilz, W. *Microporous Mater.* **1997**, *11*, 293.

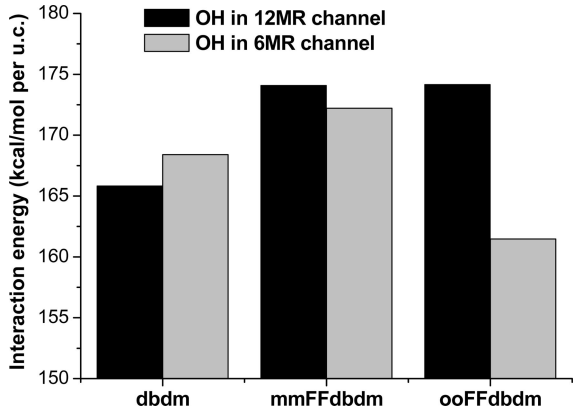

Figure 7. Total interaction energies of the different dbdm derivatives in the AFI structure. Positive charge of organic cations is compensated by hydroxide anions located in 6MR (grey) or in 12MR (black) channels.

defects and a higher concentration of hydroxide anions; in addition, these hydroxide anions are interacting with some other species. The results imply a notably larger contribution of the hydroxide anions to the charge compensation of the ooFFdbdm positive charge. These hydroxide anions should be desorbed from the structure as water at relatively high temperatures, simultaneously to the removal of the organic, in agreement with the TGA/MS experiments (Figure 4).

5. Nature and Location of the Molecules Occluded: Computational Work. We performed a subsequent computational study to explain the differences about the presence of hydroxide anions observed in the FTIR measurements. The positive charge of the organic cations is in this case explicitly compensated by the presence of hydroxide anions. Thus, we manually inserted one hydroxide anion per organic molecule. Two different locations for hydroxide anions in the AFI structure exist: in the 6MR channels, where these anions will not interact directly with the organic molecules, and in the 12MR channels, leading to appreciable interaction with the organic cations. The calculated interaction energies for the two cases are shown in Figure 7. We clearly observe that in the case of the ortho-fluorinated cation, the hydroxide anions are much more stable in the 12MR channel, very close to the organic molecule, because of a greatly stabilizing interaction between ortho-fluorine and the hydroxide anion. The lack of this stabilizing interaction in the nonfluorinated and the meta-fluorinated cations makes the location of hydroxide anions in the main channels less stable. Indeed, a higher concentration of framework defects and a lower concentration of hydroxide anions has been found for these samples in the IR study, which indicates that in these cases the creation of negatively charged framework defects to compensate the positive charge of the SDAs should be more stable than the inclusion of OH^- anions. As can be observed in Figure 7, the presence of hydroxide anions in the ooFFdbdm system increases the interaction energy. Taking this contribution into account, the calculated interaction energies of the ooFFdbdm SDA with the AFI framework is the highest among the derivatives examined, a result which explains its higher experimentally observed structure directing ability.

6. Geometry of the Occluded Hydroxide Ions. ^{27}Al MAS NMR. The question that now arises is whether these hydroxide anions inside the 12MR channels are just interacting with the organic ortho-fluorine substituent or they are also coordinated to framework aluminum atoms. To address this issue,[27]Al magic-angle spinning (MAS) NMR spectra of the SDA-containing samples were collected (Figure 8). An intense signal at around 37 ppm can be observed in all cases, corresponding to tetrahedral aluminum atoms in the AFI structure.[33] In addition, all the spectra show another broad band centered at 8 ppm, which has been assigned in the literature to unreacted pseudoboehmite or to pentacoordinated aluminum, formed by coordination of Al atoms 4-fold coordinated to framework oxygens to one water molecule. However, in the ooFFdbdm sample, there is a high contribution of another band centered at 17 ppm, which also corresponds to pentacoordinated aluminum. We tentatively assign this band to aluminum atoms coordinated to the hydroxide anions in the 12MR channel. This band dissappears when magnesium ions are introduced in the framework, leading to MgAPO materials;[32] in this case, charge balance is provided by the presence of Mg^{2+}; that is, no hydroxide anions are present, a result that supports our previous assignment. Although this band can also be observed in the dbdm and mmFFdbdm samples, its intensity is much higher in the ooFFdbdm sample, which also indicates a much higher concentration of hydroxide ions in the latter sample. Taking into account the SDA content of the samples, charge balance requirements imply that a maximum of one hydroxide anion per unit cell is present in the system. This ratio corresponds to one pentacoordinated aluminum atom out of 12 total aluminum atoms, which explains the low intensity of the resonance at 17 ppm with respect to the tetrahedral[27] Al signal. In summary, these results seem to indicate that hydroxide anions are coordinated to framework aluminum atoms, bridging the organic molecule (OH^- develops an H-bond with the ortho-fluorine atoms) and the framework (oxygen atom from OH^- coordinates to framework aluminum atoms), as depicted in Figure 9. Indeed, the development of the H-bond would weaken the O−H bond strength, explaining the red-shift observed in the FTIR spectrum of the ooFFdbdm sample.

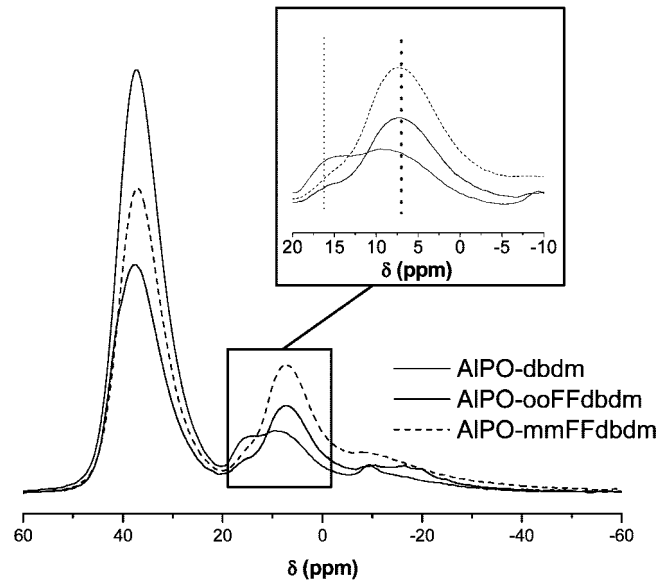

Figure 8. ^{27}Al MAS NMR spectra of the different samples.

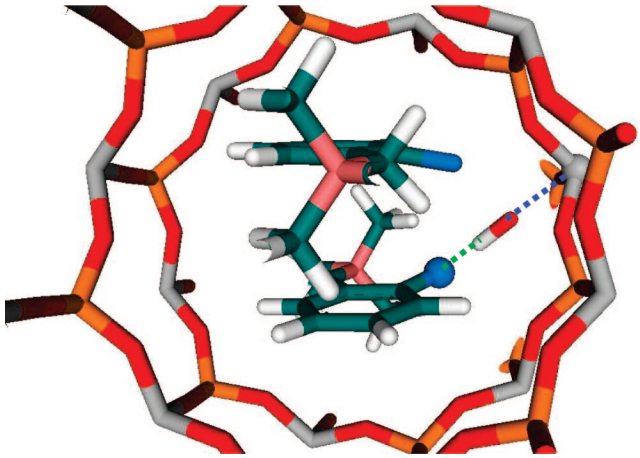

Figure 9. Model of the proposed orientation of hydroxide anions within the 12MR channels, bridging the ortho-fluorinated organic SDA and the framework. Dashed green line indicates the H-bond and dashed blue line indicates the coordination bond. Fluorine atom (blue) and pentacoordinated aluminium atom are displayed as balls.

We therefore conclude that the true SDA in the AlPO-ooFFdbdm sample is a supramolecular assembly formed between the ooFFdbdm cations and hydroxide anions. Both ions must be simultaneously incorporated during the synthesis process, giving rise in practice to a cooperative structure directing effect, because of the strong interaction between the ortho-fluorinated cation and the hydroxide anion. A similar cooperative effect was previously found for the *ortho*-fluorobenzylbenzyldimethylammonium cation and fluoride anions in the synthesis of the EUO structure.[16]

Conclusions

In this work we have examined the interaction of hydroxide anions with SDAs and the inorganic framework in the templated synthesis of the AFI-type structure. A new effect of fluorine atoms has been observed: fluorine atoms in the ortho position of dbdm promote a strong interaction with hydroxide anions during the synthesis of the AFI microporous material which results in a simultaneous incorporation of both the ooFFdbdm cation and the OH^- anion in the 12MR channel during the crystallization of the AFI structure, leading to a cooperative structure directing effect. Hydroxide anions bridge the ooFFdbdm organic cation and the framework through the development of an H-bond with the molecular ortho-fluorine substituent and by coordination with framework aluminum ions. The presence of these hydroxide anions increases notably the interaction energy of this SDA with the AFI structure and results in a higher structure directing ability.

However, when there is no fluorine in the dbdm SDA or when fluorine is located in the meta-position, there is no possibility of developing such H-bonds, and no cooperative structure directing effect occurs. Instead, dbdm and mmFFdbdm cations incorporate in the AFI structure without the simultaneous inclusion of hydroxide anions, resulting in a poorer structure directing ability. In these cases, our FTIR results indicate that charge balance to compensate the positive charge of the SDA cations is provided by the creation of negatively charged framework defects.

Acknowledgment. Financial support of the Spanish Ministry of Education and Science (Project No. CTQ2006-06282) is acknowledged. L.G.-H. acknowledges the Spanish Ministry of Education and Science for a PhD grant; F.C. is supported by an RCUK Fellowship. The authors also thank Teresa Blasco for collecting the NMR spectra, Accelrys for providing their software, and Centro Técnico de Informática (CSIC) for running the calculations.

Supporting Information Available: XRD of AlPO samples and FTIR spectra (PDF). This material is available free of charge via the Internet at http://pubs.acs.org.

CM070855B